9

Muniram Gajendra Singh Jayanthi\* and Dandinashivara Revanna Shashikumar

# Leaf Disease Segmentation From Agricultural Images via Hybridization of Active Contour Model and OFA

https://doi.org/10.1515/jisys-2017-0415 Received May 9, 2017; previously published online November 27, 2017.

**Abstract:** In this paper, an alternative active contour model (ACM) driven by an oppositional fruit fly algorithm (OFA) is presented. Unlike the traditional ACM variant, which is frequently caught in a local minimum, this methodology helps the focalizing of control points toward the global least of the energy function. In the proposed system, energy minimization is performed through a fruit fly algorithm, and every control point is compelled in a local search window. As for the local search window, the rectangular-shaped approach has been viewed. The results demonstrated that the fruit fly strategy utilizing polar coordinates is, for the most part, desirable over the fruit fly performed in rectangular shapes. Three performance metrics, such as the Jaccard index, the Dice index, and the Hausdorff distance, were utilized to validate the proposed strategy in real agricultural and synthetic images. From the results, it is clear that the proposed OFA technique shows a great option for the agricultural plant image segmentation process, considering any kind of disease that occurred in plant leaves.

**Keywords:** Active contour model, fruit fly, oppositional, energy, control pint.

# 1 Introduction

India is an agriculture country. A major portion of India's population depends on agriculture as a food source and also as an economical income [6]. Agriculture crops suffer losses due to diseases that affect plant leaves, crops, stems, and so on. If leaf infections are identified on the early premise and averted in a like manner, then, enormous misfortunes can be avoided. So, to reinforce the agricultural fields and the economy of the nation, fast and precise discovery of leaf illnesses is required [16]. With a few special cases, microscopic organisms exist as single cells and increment in numbers by separating into two cells during a procedure called binary fission. Viruses are, to a great degree, minor particles comprising of protein and hereditary material with no related protein [7]. The cost force, automatic correct-distinguishing proof, and detection of diseases based on their specific side effects get to be distinctly fundamental and extremely valuable to farmers and, furthermore, to agriculture researchers [8].

Feature extraction includes simplifying the measure of assets required to depict a huge arrangement of information accurately [12]. Analysis with an expansive number of factors generally requires a lot of memory and calculation control or an arrangement algorithm, which overfits the preparation test and sums up ineffectively to new samples [31]. Feature extraction is a general term for techniques for developing combinations of the factors to get around these issues while, as yet, portraying the information with sufficient exactness [14]. As previously, a significant number of methodologies and algorithms have been proposed in the literature, for detecting different types of features [28]: (a) edges, (b) corners, (c) geometric and morphological features, and (d) thinning and skeletonization algorithms. A color-based vision system is used to detect disease

<sup>\*</sup>Corresponding author: Muniram Gajendra Singh Jayanthi, Department of Computer Science and Engineering, Cambridge Institute of Technology, Bangalore 560036, India, e-mail: jayanthimg0679@gmail.com

Dandinashivara Revanna Shashikumar: Department of Computer Science, Cambridge Institute of Technology, Chikkabasavanapura, Krishnarajapuram, SR Layout, Bengaluru, Karnataka 560036, India; and Visvesvaraya Technological University (VTU), Jnana Sangama, Machhe, Belagavi, Karnataka 590018, India

that appears in leaves. The method can be used for real-time classification of leaves [27]. An application for feature extraction of leaves depends on the shading division, a component availability investigation, a fuzzy accumulation, and a hereditary algorithm [20].

Segmentation separates a picture into its constituent areas or objects, and it is the key step in image analysis [19]. The level to which subdivision is conveyed relies upon the issue being solved. Image segmentation algorithms depend on discontinuity and similarity, which are the fundamental properties of intensity quality [7]. To segment the image, the statistical pattern-recognition classifier was used. Good segmentation was achieved because the area can be divided by the normal area [10]. The accuracy of grading was improved, while time and cost were reduced, and for this process, hardware requirement was very low [15]. Image segmentation is the way toward relegating a label to each pixel in an image to such an extent that pixels with a similar label share certain visual attributes. Image segmentation is ordinarily used to find objects and limits that mean curves and lines in images [3].

A snake energy-minimization type approach is proposed in this paper, but based on an oppositional fruit fly algorithm (OFA), for the corn (maize) agricultural plant image segmentation. The disease, named as Northern leaf blight, occurred in the corn (maize) plant is detected by the OFA. Through a non-sequential-stage algorithm, OFA aims to find accurately targeted object edges. Local search spaces that mean windows are set at the first stage for each control point from the current contour or initial contour. Such control points inside each search window are placed randomly in the second phase to acquire new ones by the guide of the fruit fly algorithm.

The paper is organized as follows: Section 2 presents the review of the related work, and Section 3 contains the background information about the active contour model (ACM) and fruit fly optimization algorithm (FOA). Section 4 contains the motivation of this research, and Section 5 presents the proposed technique of the hybrid approach of the ACM and OFA algorithm. Section 6 provides the experimental results and discussion of the technique. Here, the data set parameters are analyzed, and the experimental results are noted. Finally, the conclusion of the proposed method is given in Section 7.

# 2 Review of Related Works

In image processing, various researchers have proposed numerous approaches for agricultural image segmentation: a handful of important researchers are offered in this segment among them. Rathod et al. [23] have examined that the agriculture research of the automatic leaf infection location was a fundamental research subject as it might demonstrate benefits in checking large fields of crops, and along these lines, consequently, identify symptoms of the disease when they appear on plant leaves. These technique studies were for increasing throughput and lessening subjectiveness emerging from human specialists in identifying the leaf disease. Digital image processing was a technique used for the enhancement of the image. Moreover, Kavitha and Ananthi [12] have explained a segmentation technique, which is used to segment the diseased portion of a leaf. In view of the segmented area texture and shading highlight, the disease can be distinguished by the arrangement system. Segmentation of the diseased region of a plant leaf was the initial phase in infection detection and identification, which assumes a vital part in agricultural research. Here, they give different segmentation methods that are utilized to segment the infected leaf of a plant.

No other than Patil and Dudhane [21] have described the detection of plant disease, and its severity was a challenging task. It relies on the image feature determination and the exactness with which the diseased portion was segmented. Here, this system was detecting disease based on content-based image retrieval (CBIR). The CBIR system is developed using the integration of color, shape, and texture features of the leaf images, while the segmentation of the diseased portion of the leaf was done using the K-means clustering algorithm. Furthermore, Sathish and Ramesh Kumar [25] explained a method for identifying plant leaf disease based on color. Agrarians are experiencing the issue rising from various sorts of plant diseases. Sometimes, biologists are also unable to identify the disease that leads to the lack of identification of the right type of disease. The input image of the leaves was converted from red green blue (RGB) to hue intensity saturation (HIS). Then, the leaf disease segmentation is done using the K-means clustering. After segmentation,

the mostly green color pixels are masked based on the specific threshold values that are computed using the Otsu's method. Here, the neural network is trained for classification.

No other than, Baghel and Jain [2] have developed the automatic detection of leaf disease, which is an essential research topic in agricultural research. Defect segmentation was done in two stages and outlines the K-means clustering technique for the segmentation of a diseased part of the leaf. To start with, the pixels were clustered based on their shading and spatial elements, where the clustering procedure was refined. At that point, the clustered blocks are converged to a particular number of regions. Moreover, Sekulska-Nalewajko et al. [26] examined an image processing strategy for the quantitative appraisal of the ROS aggregation territories in leaves stained with DAB or NBT for H<sub>2</sub>O<sub>2</sub> and O<sub>2</sub> radical dot recognition. Three types of images determined by the combination of the staining method and background color are considered. It permits selecting the stained regions of the ROS-interceded histochemical responses, in this manner, fractionated by weak, medium, and exceptional stained intensity and, therefore, ROS accumulation. It additionally assesses the total leaf sharp edge zone. Vyshnavi et al. [30] explained and diagnosed the disease using image processing and clustering techniques on the image of the plant leaf disease. The input image of the leaves was converted as RGB to HIS. At that point, leaf segmentation was done utilizing hierarchical clustering. After segmentation, for the most part, green shading pixels are covered based on particular threshold values.

# 3 Background Information

Pertinent ideas of the ACM and fruit fly algorithm are briefly described in this section.

#### 3.1 Active Contour Model: Snake

The essential thought of the ACM is the dynamic movement of a parametric bend under the action of certain control forces appearing in the image spatial zone. These forces are outlined in two sorts: internal and external forces. The internal force is dependent on the contour smoothness, and the external force is dependent on the pushing of the snake toward the protest limit. The position of the snake (ACM curve) is parametrically represented by  $P(u, v) = (a(u, v), b(u, v))^T$ , where  $u \in [0, 1]$ , and v is the discrete time between two consecutive steps. The cost capacity is the snake total energy, and its minimum is found when the snake develops near the desired contour, and that equation is given as follows:

$$Ey_{\text{snake}} = \int_{0}^{1} Ey_{\text{int}}(P(u, v) + Ey_{\text{ext}}(P(u, v)))ds$$
 (1)

where  $Ey_{int}$  is the internal energy term, and  $Ey_{ext}$  is the external energy term.

Respectively, the internal and external energy terms are described as follows:

#### Internal energy term

$$Ey_{int}(P(u, v)) = \frac{1}{2} \left[ \varepsilon(u, v) \left\| \frac{\partial P(u, v)}{\partial u} \right\|^2 + \phi(u, v) \left\| \frac{\partial^2 P(u, v)}{\partial u^2} \right\|^2 \right]$$
 (2)

where  $\varepsilon$  is the elasticity component, and  $\phi$  is the bending by the rigidity component.

#### External energy term

$$Ey_{\text{ext}}(P(u, v)) = \lambda_{\text{line}} Ey_{\text{line}}(u, v) + \lambda_{\text{edge}} Ey(u, v) + \lambda_{\text{term}} Ey_{\text{term}}(u, v)$$

$$= \lambda_{\text{line}} D(u, v) - \lambda_{\text{edge}} |\nabla G * I(P(u, v))|^{2} + \lambda_{\text{term}} \left| \frac{D_{bb} D_{a}^{2} - 2D_{ab} D_{a} D_{b} + D_{aa} D_{b}^{2}}{(D_{a}^{2} + D_{b}^{2})^{3/2}} \right|_{(u, v)}$$
(3)

where  $\lambda_{\text{line}}$ ,  $\lambda_{\text{edge}}$ ,  $\lambda_{\text{term}}$  are the external energy components.

Here, the elasticity component  $\varepsilon$ , bending by the rigidity component  $\phi$ , and the external energy by the components  $\lambda_{\text{line}}$ ,  $\lambda_{\text{edge}}$  and  $\lambda_{\text{term}}$  control the curve tension. Then, the function  $D(u, v) = G^*I(P(u, v))$  and its partial derivatives such as  $D_{y}$ ,  $D_{yy}$ ,  $D_{yy}$ ,  $D_{yy}$  and  $D_{yy}$  are the determination of the external energy term, which is composed by line  $(Ey_{line})$ , edge  $(Ey_{edge})$ , and termination  $(Ey_{term})$  energy functions. G represents the Gaussian function, and *I* represents the input image.

The customary arrangement of this issue consists of the numerical computing of the Euler condition until the balance is fulfilled.

$$\nabla E y_{\text{ext}} - \varepsilon(u, v) \frac{\partial^2 P(u, v)}{\partial u^2} + \phi(u, v) \frac{\partial^4 P(u, v)}{\partial u^4} = 0$$
(4)

This condition is comparable to the minimum energy arrangement related with the energy steadiness state. In other words, the external energy component gets to be equivalent to the internal one or the other way around.

## 3.2 Fruit Fly Algorithm

The fruit fly algorithm is a novel technique for seeking global optimization. It began from the examination of food hunting behaviors of fruit fly swarm. The fruit fly is a superb food hunter with sharp osphresis and vision. To begin with, it identifies food source by noticing a wide range of fragrances floating all around and flies going toward the corresponding place. After reaching close to the food, it might discover the food or go to that particular place with its delicate vision. Food sources are represented by the optima, and the methodology of foraging is reproduced by iteratively seeking for the optima in the FOA.

#### Steps of Fruit Fly Algorithm

1. Initialize random location of fruit fly.

Exploration using arbitrary path and detachment to the olfactory organ.

$$U_m = U_a xis + Random Value$$
  
 $V_m = V_a xis + Random Value$ 

As the food's location is unfamiliar, the distance (D) from the beginning is evaluated initially, and the computed value of the smell concentration (*C*), known as the reverse of distance, is computed next.

$$D_{m} = \sqrt{(U_{m}^{2} + V_{m}^{2})} \tag{5}$$

$$C_m = 1/D_m \tag{6}$$

Substitute the smell concentration value (*C*) into the fitness function just to detect the smell concentration (Smell<sub>m</sub>) of every fruit fly's position.

$$Smell_m = function(C_m)$$
 (7)

Detect the location of the most excellent smell concentration (highest value).

Retain the highest smell concentration value and the x, y coordinate; the fruit fly swarm will utilize visualization to flutter in that direction.

Smell Excellent = Excellent Smell

$$U_{\text{axis}} = U(\text{Excellent Index})$$
 $V_{\text{axis}} = V(\text{Excellent Index})$ 

(9)

Enter the successive optimization to replicate the execution of stages 2–5, then, decide if the smell concentration is greater than the past successive smell concentration; if yes, execute task 6.

## 4 Motivation of the Research

The image segmentation performs a significant role in the field of image processing because of its wide range of applications in the agricultural fields to identify plant diseases by segmenting the different diseases. Similarly, the automatic leaf disease segmentation is the imperative research subject in the agriculture field as it might demonstrate benefits in checking and controlling substantial fields of crops and, along these lines, consequently identify diseases when they show up on plant leaves. In the event that plant diseases are segmented on the early premise and prevented appropriately, then, huge losses can be avoided. So, to strengthen the agricultural fields and the economy of the nation, quick and exact segmentation of plant infections is required. In the last decades, many methods have been proposed to segment the disease of agricultural images such as neural network [24], Otsu's method [18], support vector machine [1], fuzzy c-means algorithm [22], K-means clustering [8], and fuzzy logic system [29]. However, segmentation of agricultural imagery remains a challenging problem due to the complexity of the images.

Moreover, ACM or Snake [11] is an energy-based technique known as one of the most powerful image segmentation methods. The basic idea of the ACM is the dynamic motion of a parametric curve under the action of certain control forces present in the image spatial domain. These forces are summarized in two types: internal and external forces. The internal force is responsible for the contour (or snake) smoothness and the external one of pushing the snake toward the object boundary. The first is the stagnation propensity in a nearby arrangement, which is said as the optimal contour rather than converging toward the optimum contour. In order to avoid this inconvenience, ACM is often initialized as close as possible to the desired or expected contour. The second drawback is related to the difficulty to converge in non-convex-shaped objects. The snake's convergence is considered as an optimization problem, in which the total energy has to become minimal so as to ensure that the snake is located on the object contour. Therefore, in order to overcome these drawbacks, the metaheuristic optimization algorithm is used which is shown in Figure 1.

# 5 Hybrid Approach of Active Contour Model and OFA Algorithm

Recently, researchers have presented different techniques for agricultural image segmentation systems. The main aim of this research is to propose the leaf disease segmentation from agricultural images via hybridization of the ACM and OFA algorithm. Here, we used the OFA for this issue. The fruit fly [32] is a novel metaheuristic swarm intelligence optimization method for solving optimization problems, which is based on the foraging behavior of the real fruit flies. In addition, opposition-based learning (OBL) will be developed to improve the candidate solution by considering the current population as well as its opposite population at the same time. In the OFA-based agricultural image segmentation, initially, we will adjust the input image for further processing. Then, we set the local search spaces (or windows) for each control point from the current contour (or initial contour, as the case may be). After that, we will place randomly such control points inside

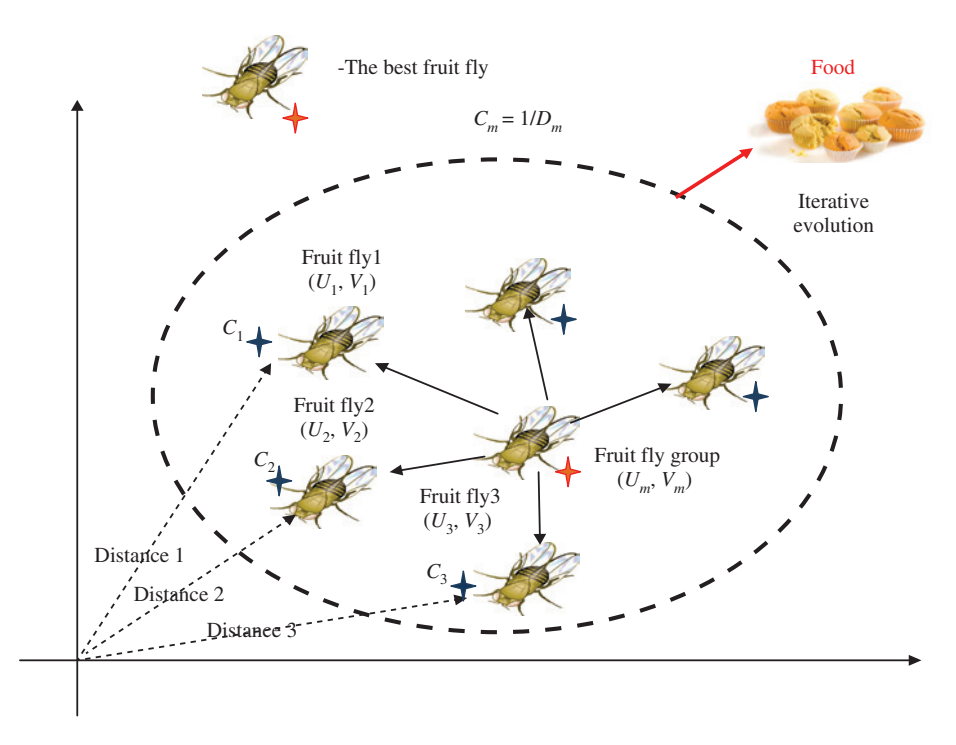


Figure 1: The Interactive Process of Group Iterative Food Searching of Fruit Fly.

each search window, in order to obtain new ones by the aid of the OFA strategy. Finally, various agricultural images are subjected to the proposed technique to evaluate the performance of segmentation.

#### **5.1 Segmentation Using Active Contour**

An active contour issue is settled customarily through a deterministic iterative strategy, for example, gradient descent [11]. To quicken the execution of the present FOA, an idea of opposition-based learning is utilized for the initial population and creating a new population in the search process. The idea behind the opposition-based learning (OBL) is the concurrent thought of an initial population and its comparing opposition population in a request to get a nearer approximation for the current population [9].

In an active contour,  $X_i$  is the  $i^{th}$  control point, and this point is represented by  $X_i(u, v) = (a(u, v), b(u, v))^T$  inside the  $i^{th}$  search window  $(SW_i)$  with  $u \in (0, 1)$ , and v is the time. Then, with the  $j^{th}$  candidate in the  $i^{th}$  search window, the control point is mentioned by  $q_i$ .

In a given search window, the local energy function of each candidate is defined as [12]

$$Ey_{i,j} = \frac{1}{2} (\varepsilon || X_{i+1} - Y_{i,j} ||^2 + \phi || X_{i+1} - 2Y_{i,j} + X_{i-1} ||^2)$$

$$= \lambda_{\text{line}} D(X_{i,j}) - \lambda_{\text{edge}} |\nabla G * I(Y_{i,j})|^2 + \lambda_{\text{term}} \left| \frac{D_{bb} D_a^2 - 2D_{ab} D_a D_b + D_{aa} D_b^2}{(D_a^2 + D_b^2)^{3/2}} \right|_{Y_{i,j}}$$
(10)

where  $\varepsilon$ ,  $\phi$ ,  $\lambda_{\text{line}}$ ,  $\lambda_{\text{edge}}$  and  $\lambda_{\text{term}}$  are weight factors, and at the candidate position  $q_{i,j}$ , the external energy components are evaluated through an interpolation process. The optimization problem for each search window can be set by  $Ey_{i,j}$  [12]:

$$B_i = \arg_i \min\{Ey_{i,j}\}, j \in \{1, ..., C_n\} \subset Sw_i$$
 (11)

where,  $B_i$  is the best index and  $C_n$  is the number of candidate in a search window i.

Therefore,  $i^{\text{th}}$  control point can be updated with  $Y_i$ ,  $B_i$ , and hence,  $P_i = Y_i$ ,  $B_i$ . Here, Ref. [31] can be solved for all  $C_n$  of the active contour using the FOA. Therefore, the total energy is estimated using the following equation [14]:

$$Ey_{\text{snake}} \approx \sum_{i=1}^{C_n} Ey_{i,B_i} \tag{12}$$

where  $Ey_{i,R}$  is the best candidate with minimum local energy.

Finally, until the total snake energy gets to be stable, the above process is repeated, i.e. the energy value remains the same or decreases marginally per every repetition.

## 5.2 OFA (Oppositional Fruit Fly Algorithm)

**Data:** FOA method and initial active contour snake.

Result: Best active contour

- Step 1: Parameter initialization: the main parameters of the FOA are the total evolution number and the population size. In our suggested technique, the fruit fly represents the initial active contour points. Initialize the random location of the fruit fly (*EyU*\_axis, *EyV*\_axis).
- Step 2: To modify the traditional fruit fly algorithm, the oppositional method is introduced. Here, the opposite agent's positions  $(OB_i)$  are completely defined by the components of  $B_i$

$$OB_{i} = [ob_{i}1, \dots, ob_{i}C_{n}]$$

$$(13)$$

where  $ob_i = \text{Low}_i + \text{Up}_i - b_i$  with  $ob_i \in [\text{Low}_i, \text{Up}_i]$  as the position of the  $i^{\text{th}}$  opposite agent  $OB_i$  in the  $d^{\text{th}}$  dimension of the oppositional population.

- **Step 3**: Exploration using arbitrary path and detachment to the olfactory organ. Here,  $X_i$  is the  $i^{th}$  control point of the active contour.

$$X_{i}(u, v) = (EyU_{m}, EyV_{m})^{\mathrm{T}}$$
(14)

$$EyU_m = EyU_axis + Random Value$$
  
 $EyV_m = EyV_axis + Random Value$ 

- Step 4: Fitness evaluation

$$C_m = B_i \tag{15}$$

$$B_{i} = \arg_{i} \min\{Ey_{i,j}\}, j \in \{1, ..., C_{n}\} \subset Sw_{i}$$
 (16)

Step 5: Substitute the smell concentration value (*C*) into the fitness function just to detect the smell concentration (Smell\_\_) of every fruit fly's position.

$$Smell_{m} = function(min C_{m})$$
 (17)

Step 6: Detect the location of the most excellent smell concentration (highest value).

$$[Excellent Smell Excellent Index] = High (Smell)$$
(18)

- **Step 7**: Retain the highest smell concentration value and the *x*, *y* coordinates; the fruit fly swarm will utilize visualization to flutter in that direction.

EyU\_axis = EyU(Excellent Index) EvV axis = EvV(Excellent Index)

- **Step 8:** Enter the successive optimization to replicate the execution of stages 3–6, then, decide if the smell concentration is greater than the past successive smell concentration; if yes, execute task 6.

Finally, after getting the minimum snake energy value, we estimate the active contour model in the image segmentation as shown in Figure 2.

# **6 Experimental Result and Discussion**

The results talked about in this section were acquired from the proposed strategy implemented in a PC with the accompanying details: CPU Intel® Pentium 1.9 GHz, 64-bit operating system, Microsoft® Windows 10, 4 GB of RAM, and Math Works Matlab R2014b stage. To start with, all tests were performed for an arrangement of leaf disease segmentation from agricultural images. Here, the agricultural plant corn (maize) is taken, and the northern leaf blight disease is segmented which is shown in Figure 3. In order to take this plant's image, the online stage dedicated to crop health and crop infections, called Plant Village (https://www.plantvillage.org/en/plant\_images) dataset, is used.

## **6.1 Quality Metrics**

To evaluate the clustering performance, the proposed method uses different types of measures such as the Jaccard coefficient (J), Dice's coefficient (D), Hausdorff distance (dH), time (s), and position.

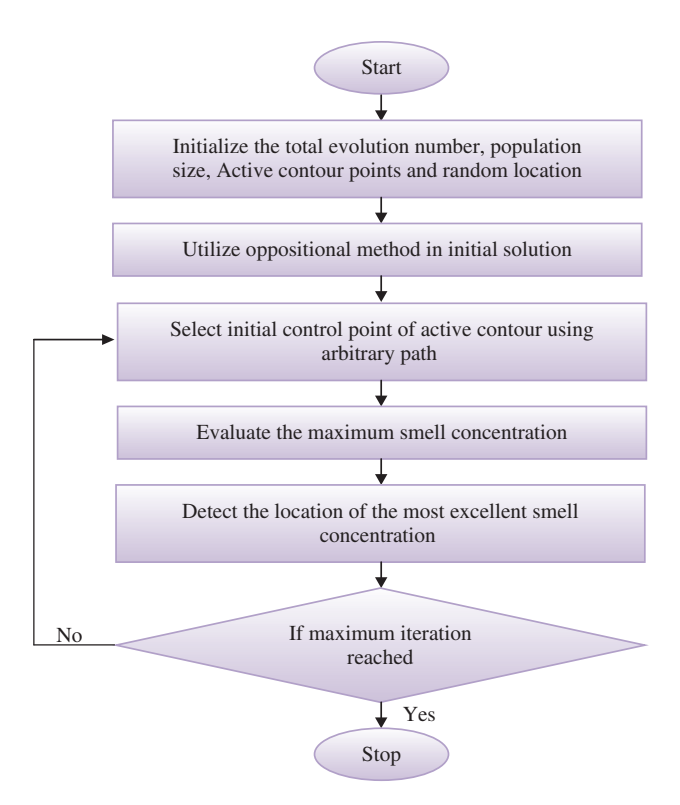


Figure 2: Flow Diagram of the Proposed OFA.

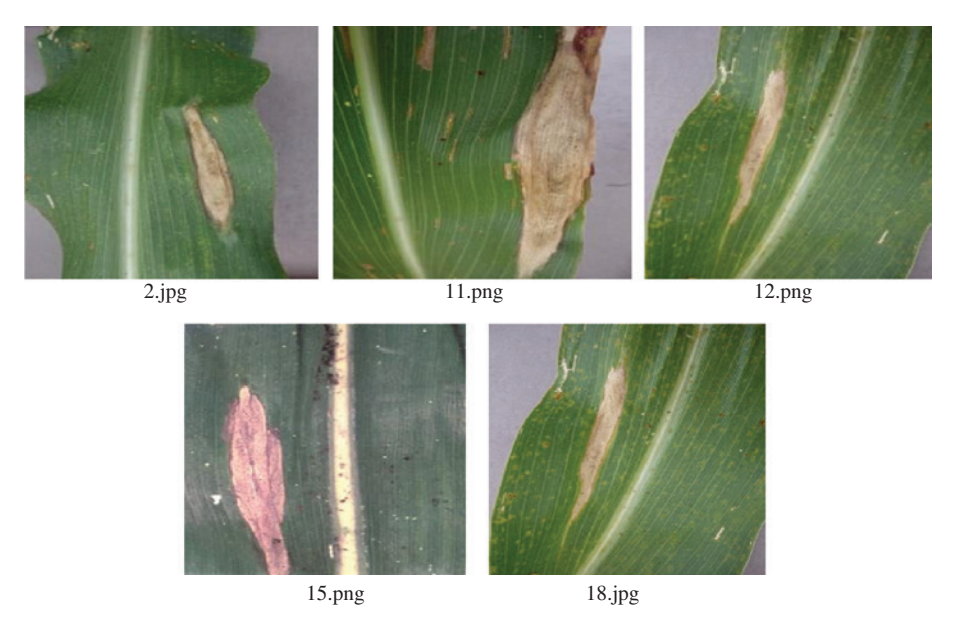


Figure 3: Input Images of Agricultural Plant Corn (maize) from the Dataset.

#### 6.1.1 Jaccard Coefficient

The J measures the similarity between finite sample sets and is defined as the size of the intersection divided by the size of the union of the sample sets.

$$J(S_1, S_2) = \frac{|S_1 \cap S_2|}{|S_1 \cup S_2|} = \frac{|S_1 \cap S_2|}{|S_1| + |S_2| - |S_1 \cap S_2|}$$
(20)

If  $S_1$  and  $S_2$  are both empty,  $J(S_1, S_2) = 1$ . Otherwise,  $0 \le J(S_1, S_2) \le 1$ .

#### 6.1.2 Dice's Coefficient

The Dice score is regularly used to evaluate the execution of the image segmentation techniques. Then, the comment on some ground truth area in the image and after that makes a computerized algorithm to do it.

$$D(S_1, S_2) = \frac{2|S_1 \cap S_2|}{|S_1| + |S_2|}$$
(21)

#### 6.1.3 Hausdorff Distance

The maximum distance of a set to the closest point in the other set is known as the Hausdorff distance. The Hausdorff distance from set *X* to set *Y* is a maximin function, defined as

$$h(X, Y) = \max_{x \in X} \left\{ \min[E(x, y)] \right\}$$
 (22)

where

x and y are the points of sets X and Y, respectively, and E(x, y) is any metric between the x and y points. For simplicity, E(x, y) is taken as the Euclidean distance between x and y.

## 6.2 Criteria for Evaluating the Performance

Here, in this proposed method, FOA is used, and the *J*, *D*, *dH*, time, and position of the image is calculated using the ACM strategy which is shown in Figure 4. Further, the same images were processed with the genetic algorithm and without using any optimization technique for the same measures such as the *J*, *D*, *dH*, time, and position. While comparing the values of the three techniques, our proposed method, FOA (Table 1) values show the better performance than the existing genetic algorithm (Table 2) and without the optimization technique (Table 3). In Figure 5, the accuracy values of the different plant images were calculated for the proposed OFA-based ACM technique, existing GA-based ACM, region scalable ACM with global constraint (RSGC) [5], region scalable fitting model (RSF) [13], ACM without edges (CV) [4], and conventional ACM method.

In this section, the experimental results are analyzed with various agricultural plant images. The output result of image 2.jpg is given in Figure 6, and the proposed method is compared with the existing GA and without the optimization technique. Here, (A) is the output result of the proposed OFA-based ACM method, (B) is the output result of the existing GA-based ACM, and (C) is the output result without using the optimization technique, i.e. the conventional ACM method. In Figure 6, first, the input image 2.jpg is initialized, and it is processed with 250 iterations. The initialization of the input image is done by taking the position value. The position of the image is chosen randomly as X-min, X-max, Y-min, and Y-max, and then, the segmented area is selected. For each and every algorithm, the position value such as X-min, X-max, Y-min, and Y-max is changed. To improve the robustness and to reflect the effectiveness of the proposed algorithm, the rule is obtained for the initialization of the test images. That is, the value of X-max should be greater than X-min, and the

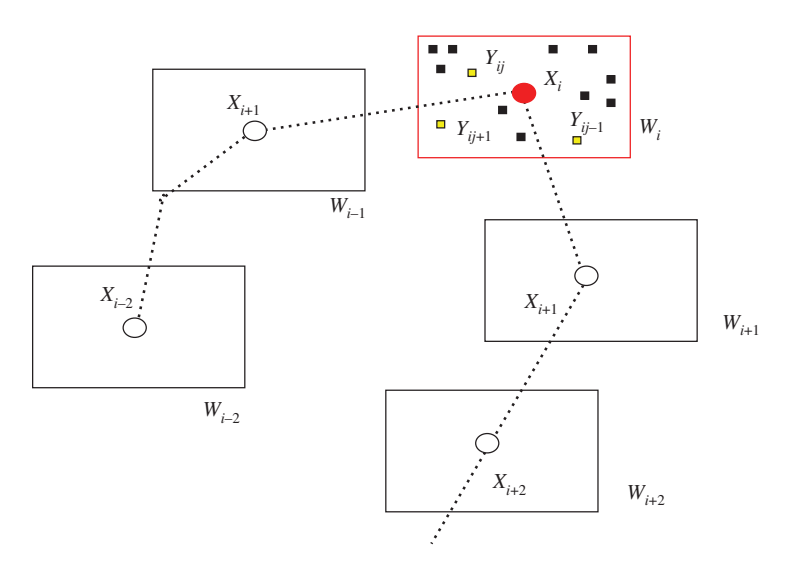


Figure 4: The ACM.

Table 1: Performance Analysis Using the Proposed OFA-based ACM.

lmage name	Jaccard coefficient	Dice coefficient	Hausdorff distance	Time	Position				
					X-min	X-max	Y-min	<i>Y</i> -max	
2.jpg	0.912834382	0.16035389	16.58312395	3.756861	300	600	70	100	
11.png	0.797462104	0.33685075	15.96871942	5.084456	10	700	250	350	
12.png	0.975752784	0.047346414	20	5.33972	50	550	200	250	
15.png	0.978901554	0.041324998	18.1934054	5.659295	250	750	280	400	
18.jpg	0.963663067	0.070125713	20.39607805	5.44846	40	600	200	230	

Table 2: Performance Analysis Using Existing GA.

Image name	Jaccard coefficient	Dice coefficient	Hausdorff distance	Time	Position				
					X-min	X-max	Y-min	<i>Y</i> -max	
2.jpg	0.912199666	0.161427298	16.58312395	3.809038	200	400	70	90	
11.png	0.8098725	0.319507783	15.96871942	5.065209	100	700	250	300	
12.png	0.976566434	0.045794016	20	5.453686	250	500	210	240	
15.png	0.979097462	0.040949135	18.1934054	5.557844	200	450	280	400	
18.jpg	0.968258999	0.061529011	20.39607805	5.46405	70	400	150	230	

Table 3: Performance Analysis without the Optimization Technique.

Image name	Jaccard coefficient	Dice coefficient	Hausdorff distance	Time	Position				
					X-min	X-max	<i>Y</i> -min	<i>Y</i> -max	
2.jpg	0.912172484	0.161473238	16.58312395	3.694212	200	400	50	70	
11.png	0.799492692	0.33403763	15.96871942	5.116356	70	600	250	340	
12.png	0.979605023	0.039974671	20	5.433854	300	350	200	230	
15.png	0.986819508	0.026018053	18.1934054	5.399891	250	400	280	400	
18.jpg	0.968223338	0.061596008	20.39607805	5.640454	100	400	150	230	

value of  $Y_{\max}$  should be greater than  $Y_{\min}$ . These  $X_{\min}$ ,  $X_{\max}$ ,  $Y_{\min}$ , and  $Y_{\max}$  values should not be greater than the image size (width and height). Then, the value of  $X_{\min}$ ,  $X_{\max}$ ,  $Y_{\min}$ , and  $Y_{\max}$  should not be <1. For image 2.jpg, when using the proposed OFA algorithm, the initialization position values are X-min=300, X-max=600, Ymin = 70, and Y-max = 100. Similarly, using the existing GA algorithm, the initialization position values are Xmin = 200, X-max = 400, Y-min = 70, and Y-max = 90. Then, by applying without the optimization technique, the initialization position values are X-min = 200, X-max = 400, Y-min = 50, and Y-max = 70. Finally, the global region-based segmentation using the ACM is experimented with greater accuracy.

Similarly, in Figure 7, the input image 11.png is segmented using the proposed OFA, existing GA, and without using the optimization technique. For image 11,png, when using the proposed OFA-based ACM algorithm, the initialization position values are X-min = 10, X-max = 700, Y-min = 250, and Y-max = 350. Similarly,

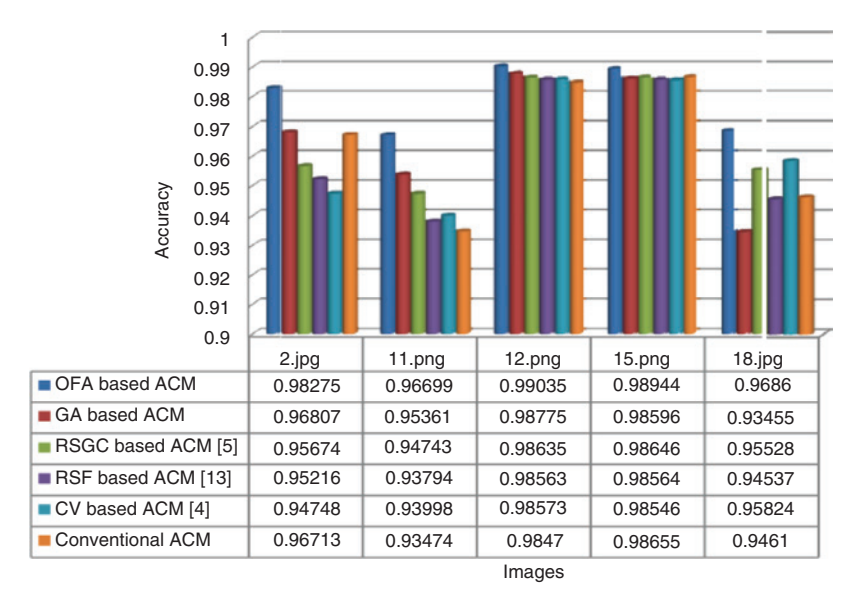


Figure 5: The Accuracy Comparison between the Proposed OFA-based ACM, GA-based ACM, RSGC, RSF, CV, and conventional ACM.

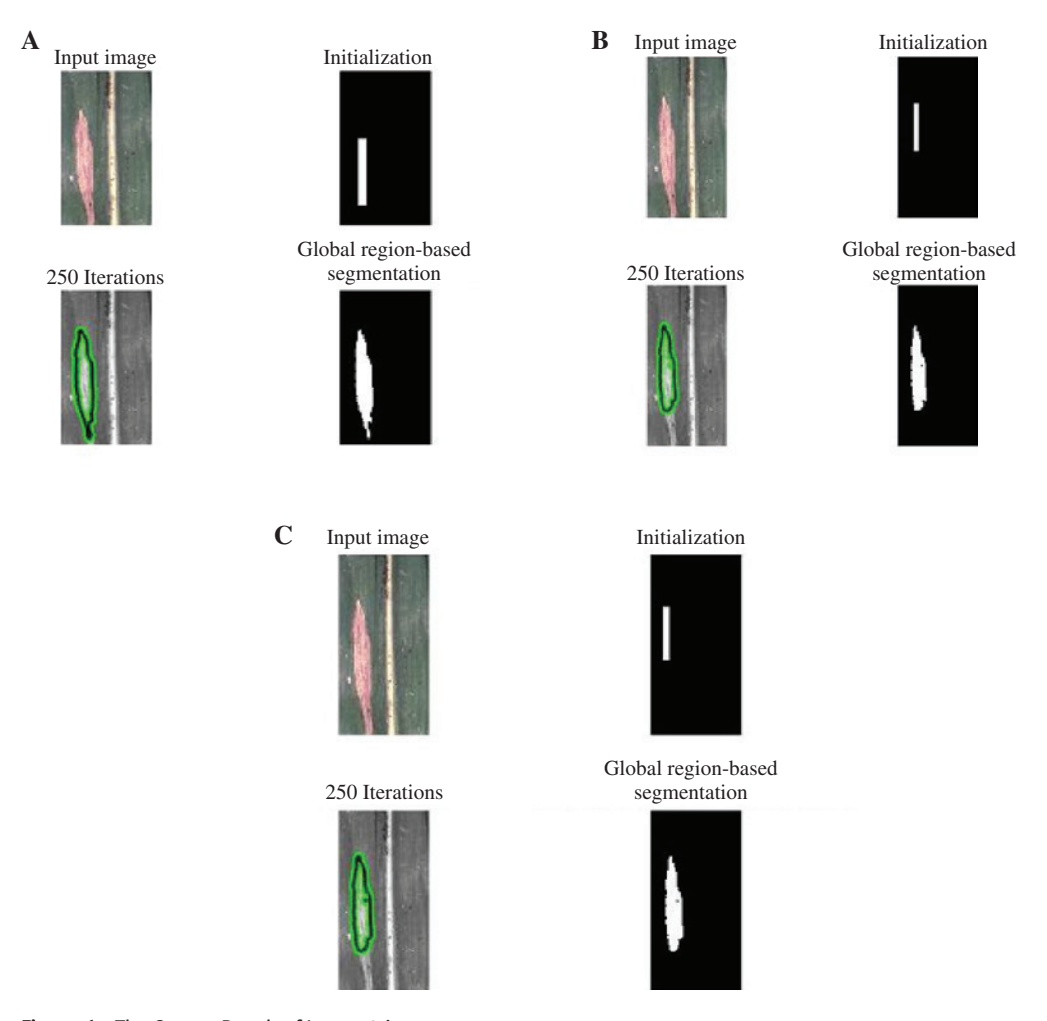


Figure 6: The Output Result of Image 2.jpg.
(A) Proposed OFA-based ACM; (B) GA-based ACM; (C) conventional ACM.

using the existing GA-based ACM algorithm, the initialization position values are X-min = 100, X-max = 700, Y-min = 250, and Y-max = 300. Then, by applying the conventional ACM technique, the initialization position values are X-min = 70, X-max = 600, Y-min = 250, and Y-max = 340.

Likewise, in Figure 8, the input image 12.png is segmented using the proposed OFA-based ACM, GA-based ACM, and conventional ACM technique. For image 12.png, when using the proposed OFA-based ACM algorithm, the initialization position values are X-min = 50, X-max = 550, Y-min = 200, and Y-max = 250. Similarly, using the existing GA-based ACM algorithm, the initialization position values are X-min = 250, X-max = 500, Y-min = 210, and Y-max = 240. Then, by applying conventional ACM technique, the initialization position values are X-min = 300, X-max = 350, Y-min = 200, and Y-max = 400.

Also, in Figure 9, the input image 15.png is segmented using the proposed OFA, existing GA, and without using the optimization technique. For image 15.png, when using the proposed OFA-based ACM algorithm, the initialization position values are X-min=250, X-max=750, Y-min=280, and Y-max=400. Similarly, using the GA-based ACM algorithm, the initialization position values are X-min=200, X-max=450, Y-min=280, and Y-max=400. Then, by applying the conventional ACM technique, the initialization position values are X-min=250, X-max=400, Y-min=150, and Y-max=230.

The same as above, in Figure 10, the input image 18.png is segmented using the proposed OFA-based ACM, GA-based ACM, and conventional ACM technique. For image 18.jpg, when using the proposed OFA-based ACM algorithm, the initialization position values are X-min = 40, X-max = 600, Y-min = 200, and Y-max = 230.

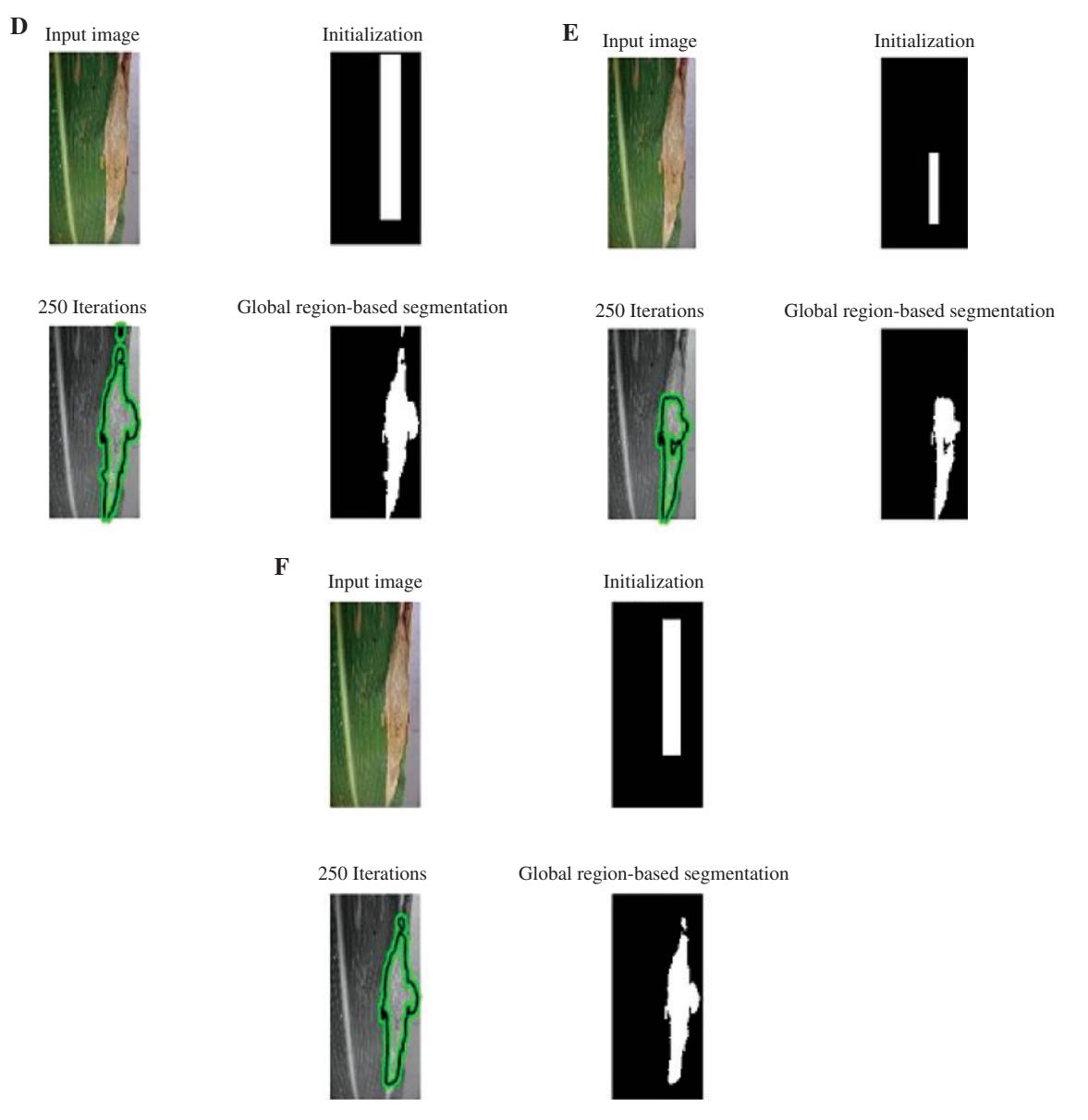


Figure 7: The Output Result of Image 11.png. (D) Proposed OFA-based ACM; (E) GA-based ACM; (F) conventional ACM.

Similarly, using the GA-based ACM algorithm, the initialization position values are X-min=70, X-max=400, Y-min = 150, and Y-max = 230. Then, by applying the conventional ACM technique, the initialization position values are X-min = 100, X-max = 400, Y-min = 150, and Y-max = 230.

The segmentation accuracy value is calculated for various images such as the accuracy value of the proposed OFA-based ACM, existing GA, RSGC, RSF, CV, and conventional ACM. The average value for the proposed OFA-based ACM method is 0.979626, for the GA-based ACM method, 0.965988, for the RSGC-based ACM, 0.966452, for the RSF-based ACM, 0.961348, for the CV-based ACM, 0.963378, and for the conventional ACM process, the accuracy value is 0.963844. Therefore, by comparing the average values, our proposed OFAbased ACM is more effective than the other existing methods.

Table 1 describes the performance of the proposed OFA technique. While taking image 2.jpg, the J value is 0.912, then, using the D, the value is 0.1603, and the dH value is 16.583. The time taken to process this image is 3.7568 s. For image 11.png, the *J* value is 0.7974, and for the *D*, the value is 0.336. Then, calculating

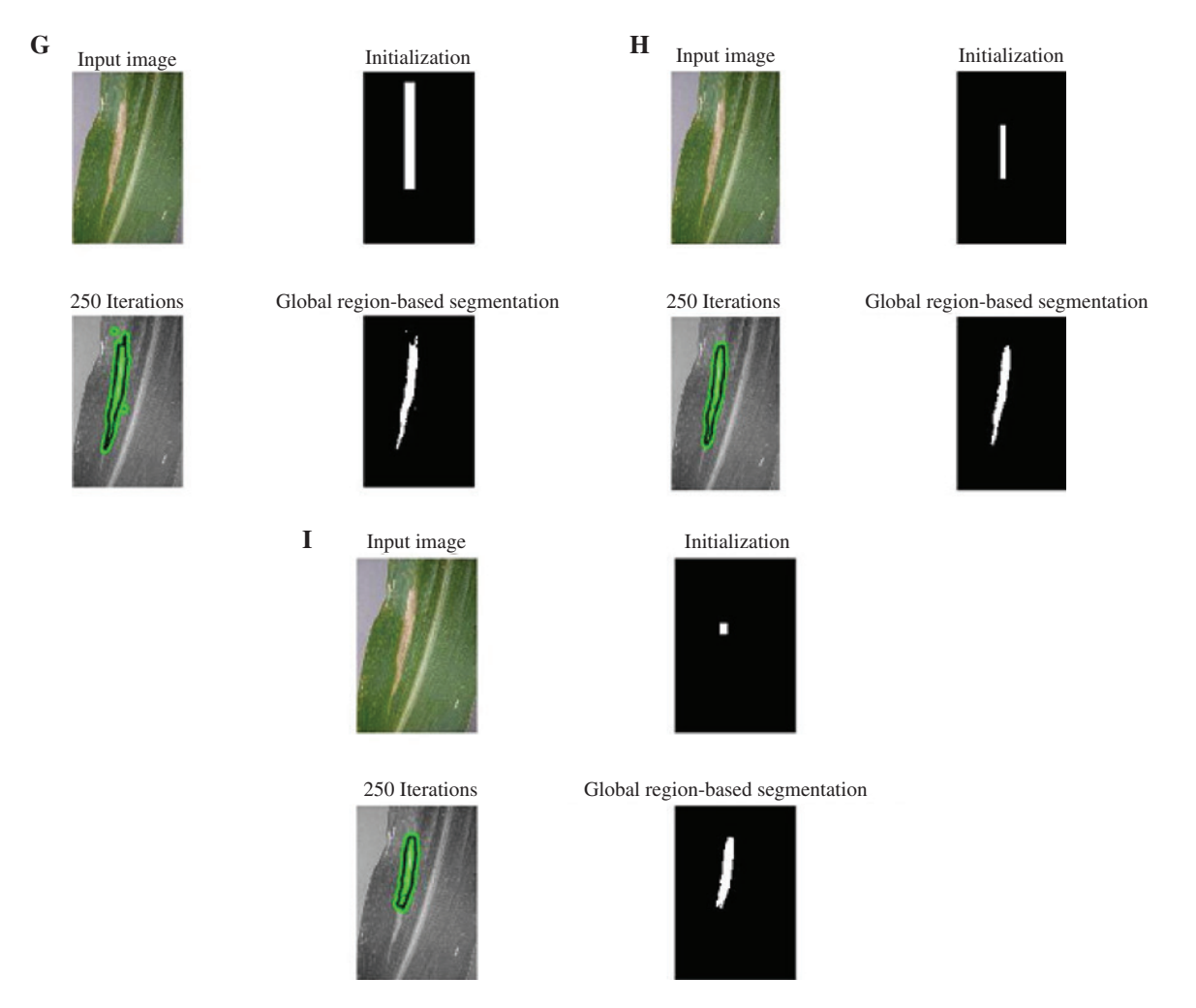


Figure 8: The Output Result of Image 12.png.
(G) Proposed OFA-based ACM; (H) GA-based ACM; (I) conventional ACM.

the dH, the value is 15.968, and the time is 5.084 s. For image 12.png, the J is 0.97575, the D value is 0.0473, and the dH is 20. The performance time is 5.33972 s. Then, the next image, 15.png, is taken and analyzed for certain calculations such as the J, and its value is 0.97890. Then, for the D, the value is 0.04132, and for the dH, the value is 18.193. The time taken to process the image is 5.659295 s. Finally, for image 18.jpg, the J value is 0.9636, for the D, the value is 0.0701, and for the dH, the value is 20.39. The time taken in processing this image is 5.44846 s.

Table 2 describes the performance of the existing GA. Taking image 2.jpg, the J value is 0.912, then the D value is 0.3195, and the dH value is 16.583. The time taken for the processing of this image is 3.8090 s. For image 11.png, the J value is 0.8098, and for the D, the value is 0.3195. Then, calculating for dH, the value is 15.968, and the time is 5.065 s. For image 12.png the J is 0.9765, the D value is 0.0457, the dH is 20. The performance time is 5.4536 s. Then, the next image 15.png is taken and analyzed for certain calculations such as the J, and its value is 0.9790. Then, for the D, the value is 0.0409, and for the dH, the value is 18.193. The time taken to process the image is 5.557844 s. Finally, for image 18.jpg, the J value is 0.9682, the D value is 0.0615, and the dH value is 20.396. The time taken in processing this image is 5.46405 s.

Table 3 describes the performance without using the optimization technique. For image 2.jpg, the *J* value is 0.912, then the *D* value is 0.1614, and the *dH* value is 16.5831. The time taken for this image to be processed is 3.6942 s. For image 11.png, the *J* value is 0.7994, and the *D* value is 0.33340. Calculating for

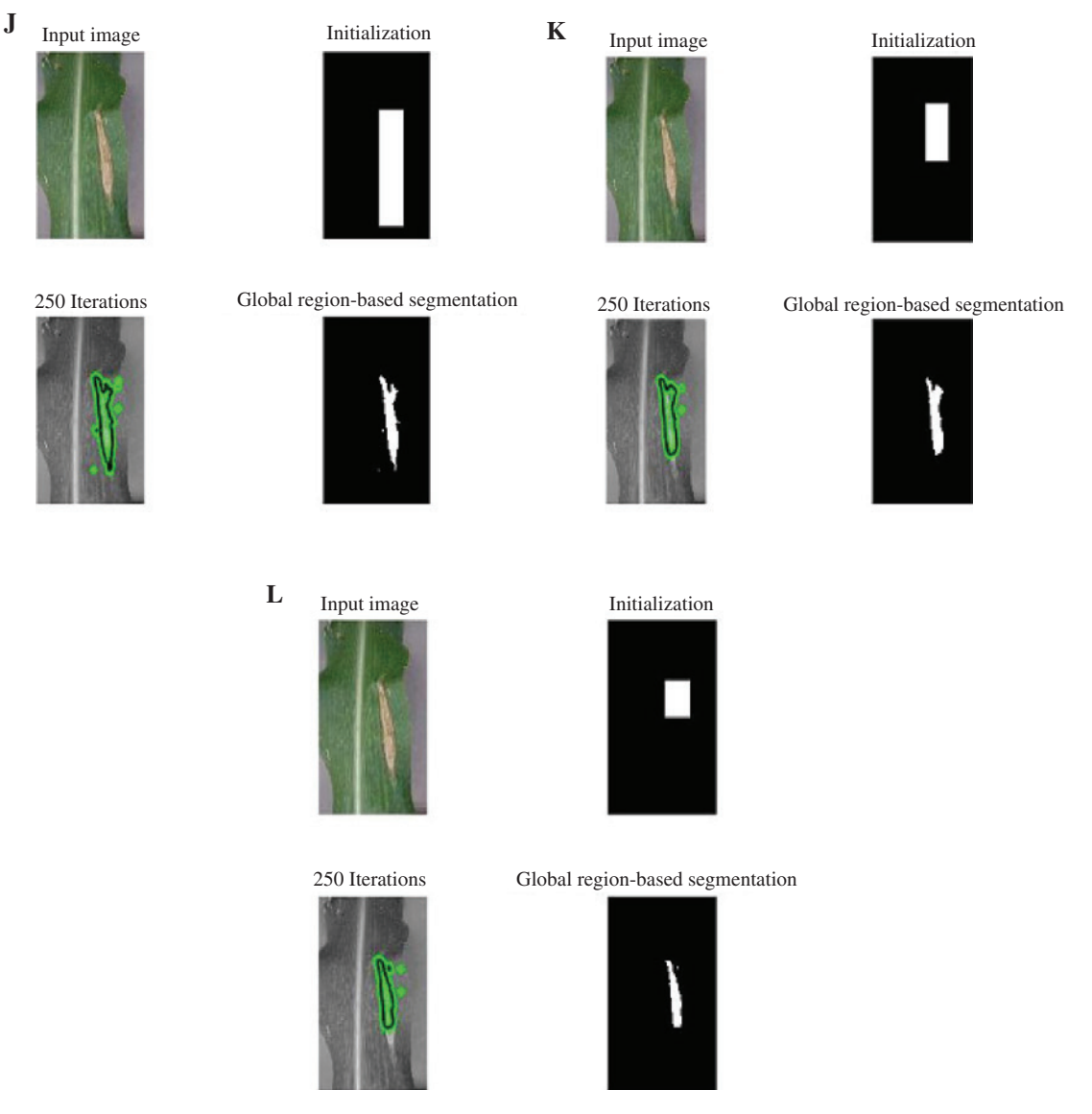


Figure 9: The Output Result of Image 15.png. (J) Proposed OFA-based ACM; (K) existing GA-based ACM; (L) conventional ACM.

*dH*, the value is 15.9687, and the time is 5.1163 s. For image 12.png, the *J* is 0.9796, the *D* value is 0.0399, and the *dH* is 20. The performance time is 5.3998 s. Then, the next image 15.png is taken and analyzed for certain calculations such as the *J*, and its value is 0.9868. Then, for the *D*, the value is 0.0260, and for the dH, the value is 18.1934. The time taken to process the image is 5.399891 s. Finally, for image 18.jpg, the J value is 0.9682, the *D* value is 0.0615, and the *dH* value is 20.3960. The time taken in processing this image is 5.640454 s.

# 6.3 Comparative Analysis

In Figure 11, we compared the performance of the precision and recall value by the proposed and existing ACM [17].

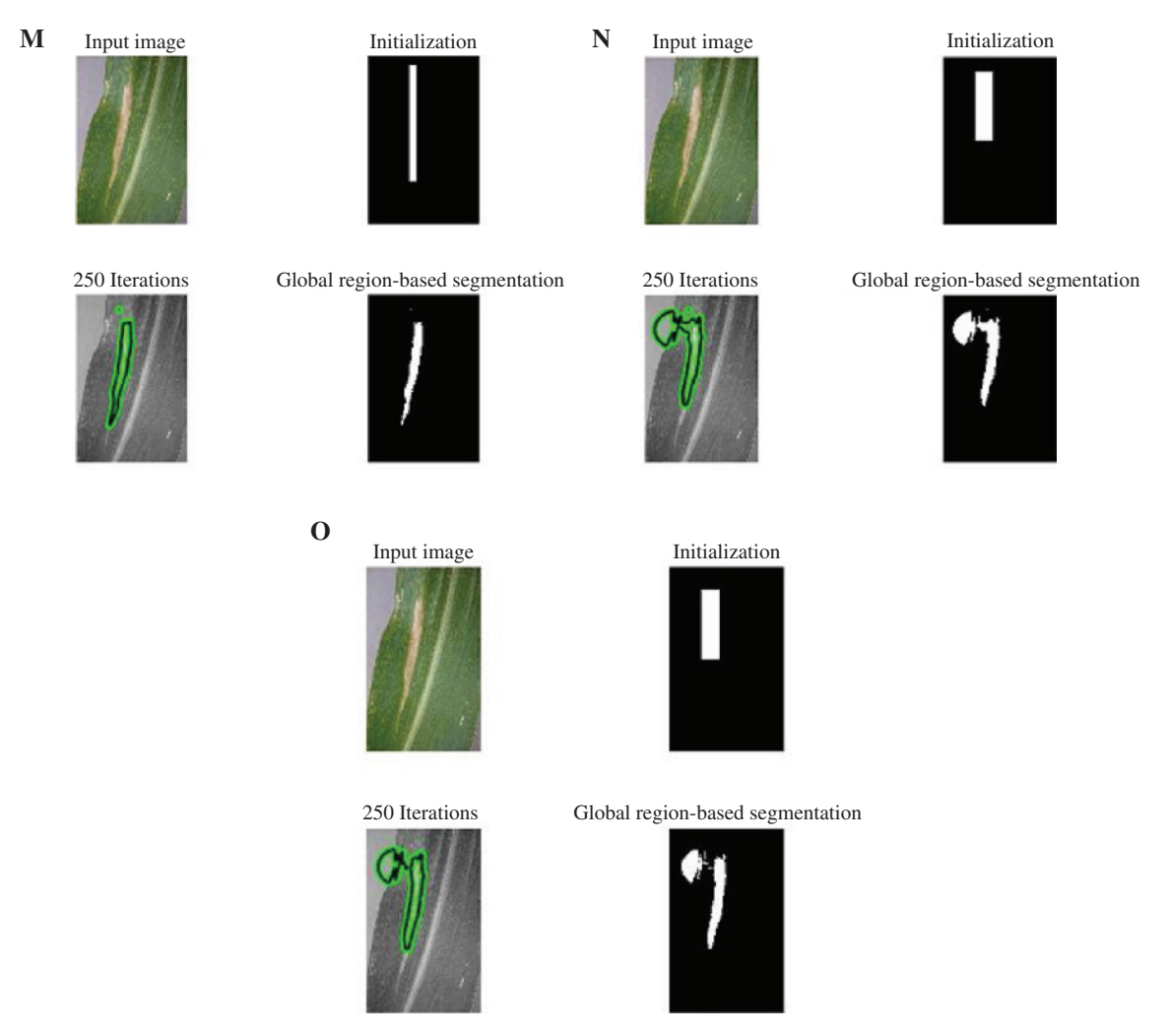


Figure 10: The Output Result of Image 18.jpg.
(M) Proposed OFA-based ACM; (N) existing GA-based ACM; (O) conventional ACM.

While absorbing the plot, the precision value of the proposed OFA method is 98.26 and that of the existing ACM method is 97.08. Further, upon comparison, the recall value of the proposed OFA method is 97.48 and that of the existing ACM method is 95.86. Hence, our proposed OFA value is greater than that of the existing ACM method.

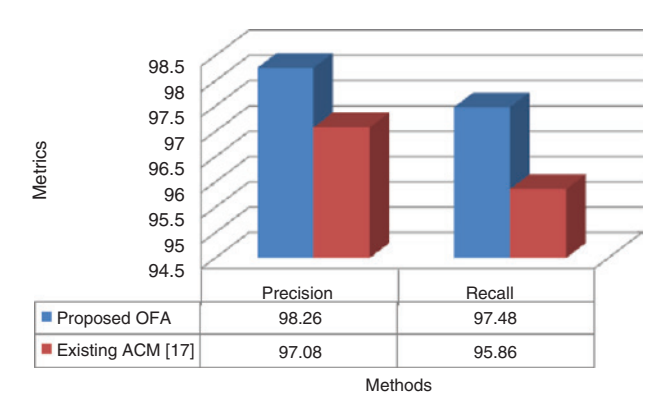


Figure 11: Comparative Analysis of Precision and Recall Values.

# 7 Conclusion

In this work, an OFA is used to solve the snake energy minimization problem for the image segmentation. The OFA was successfully implemented and tested on leaf images. Many leaf diseases were identified and analyzed. The OFA is an alternative approach to the traditional ACM, which is usually solved by the gradient descent method as described earlier. In this proposed technique, the OFA in the search window overcomes the traditional snake drawbacks, which, in turn, is overcome by the new ACM. This means that the stagnation propensity in a neighborhood and the trouble to join in non-convex formed objects is least. The OFA can usually discover solutions effectively, and it can be identified from the test results. Using the related fruit fly quantity, the stability of the fruit fly swarm search route is identified clearly. The results demonstrated that the ACM driven by the OFA is more efficient than the original form. Likewise, the ACM guided by the OFA was actualized for the purpose of comparison. The outcomes revealed that the proposed approach beats the relative ACM driven by the OFA. It was seen that the proposed OFA technique shows a powerful option for the agricultural plant image segmentation process, considering any sort of disease that occurred in the plant leaves.

# **Bibliography**

- [1] F. Ahmed, H. Abdullah Al-Mamun, A. S. M. Hossain Bari, E. Hossain and P. Kwan, Classification of crops and weeds from digital images: a support vector machine approach, J. Crop Prot. 40 (2014), 98-104.
- [2] J. Baghel and P. Jain, K-means segmentation method for automatic leaf disease detection, Int. J. Eng. Res. Appl. 6 (2016),
- [3] J. Cai, M. Golzarian and S. Miklavcic, Novel image segmentation based on machine learning and its application to plant analysis, IJIEE 1 (2011), 79-84.
- [4] T. F. Chan and L. A. Vese, Active contours without edges, IEEE Trans. Image Process. 10 (2001), 266-277.
- [5] Y. Chen, X. Yue, R. Y. Da Xu and H. Fujita, Region scalable active contour model with global constraint, Knowl. Based Syst. **120** (2017), 57-73.
- [6] A. Darshana, J. Majumdar and S. Ankalaki, Segmentation method for automatic leaf disease detection, Int. J. Innov. Res. Comput. Commun. Eng. 3 (2015), 7271-7282.
- [7] S. B. Dhaygude and N. P. Kumbhar, Agricultural plant leaf disease detection using image processing, Int. J. Adv. Res. Electr. Electron. Instrum. Eng. 2 (2013), 599-602.
- [8] S. R. Dubey, P. Dixit, N. Singh and J. P. Gupta, Infected fruit part detection using K-means clustering segmentation technique, Int. J. Artif. Intell. Interact. Multimed. 2 (2013), 65-72.
- [9] N. Gouthamkumar, V. Sharma and R. Naresh, An oppositional learning based gravitational search algorithm for short term hydrothermal scheduling, A/CEM 4 (2015), 45-54.
- [10] H. P. Kanjalkar and S. S. Lokhande, Feature extraction of leaf diseases, Int. J. Adv. Res. Comput. Eng. Technol. (IJARCET) 3 (2014), 153-155.
- [11] M. Kass, A. Witkin and D. Terzopoulos, Snakes: active contour models, Int. J. Comput. Vis. 1 (1998), 321-331.
- [12] P. Kavitha and B. Ananthi, Segmentation of unhealthy region of plant leaf using image processing techniques: a survey, Int. J. Res. Eng. Technol. 3 (2014), 1.
- [13] C. Li, C.-Y. Kao, J. C. Gore and Z. Ding, Minimization of region-scalable fitting energy for image segmentation, IEEE Trans. Image Process. 17 (2008), 1940-1949.
- [14] Y. Li, Z. Chi and D. Feng, Leaf vein extraction using independent component analysis, in: Proc. IEEE International Conference on Systems, Taipei, Taiwan, pp. 3890-3894, 2006.
- [15] H. Marathe and P. Kothe, Leaf disease detection using image processing technique, Int. J. Eng. Res. Technol. (IJERT) 2 (2013), ISSN: 2278-0181.
- [16] R. Masood, S. A. Khan and M. N. A. Khan, Plants disease segmentation using image processing, Int. J. Mod. Educ. Comput. Sci. 1 (2016), 24-32.
- [17] M. Minervini, M. M. Abdelsamea and S. A. Tsaftaris, Image-based plant phenotyping with incremental learning and active contours, Ecol. Inform. 23 (2014), 35-48.
- [18] A. Mizushima and R. Lu, An image segmentation method for apple sorting and grading using support vector machine and Otsu's method, J. Comput. Electron. Agric. 94 (2013), 29–37.
- [19] R. G. Mundada and V. V. Gohokar, Detection and classification of pests in green house using image processing, IOSR J. Electron. Commun. Eng. (IOSR-JECE) 5 (2013), 57-63.

- [20] J. C. Neto, G. E. Meyer and D. D. Jones, Individual leaf extractions from young canopy images using Gustafson-Kessel clustering and a genetic algorithm, Comput. Electron. Agric. 51 (2006), 66-85.
- [21] S. B. Patil and T. M. Dudhane, Leaf disease severity detection using K-means clustering and CBIR, Int. Res. J. Eng. Technol. (IRJET) 2 (2015).
- [22] V. Premalatha, M. G. Sumithra, S. Deepak and P. Rajeswari, Implementation of spatial FCM for leaf image segmentation in pest detection, Int. J. Adv. Res. Comput. Sci. Softw. Eng. 4 (2014).
- [23] A. N. Rathod, B. Tanawal and V. Shah, Image processing techniques for detection of leaf disease, Int. J. Adv. Res. Comput. Sci. Softw. Eng. 3 (2013), 397-399.
- [24] R. Sammouda, N. Adgaba, A. Touir and A. Al-Ghamdi, Agriculture satellite image segmentation using a modified artificial Hopfield neural network, Comput. Human Behav. 30 (2014), 436-441.
- [25] V. Sathish and K. Ramesh Kumar, Identification and classification of plant leaf disease, Int. J. Adv. Res. Sci. Eng. IJARSE 4 (2015).
- [26] J. Sekulska-Nalewajko, J. Goclawski and J. Chojak-Kozniewska, Automated image analysis for quantification of reactive oxygen species in plant leaves, Methods 109 (2016), 114-122.
- [27] A. Srivastava, M. Shugen and I. Kousuke, Development of a sensor for automatic detection of downey mildew disease, in: International Conference on Intelligent Mechatronics and Automation (ICIMA 2004), Chengdu, China, pp. 562-567, 2004.
- [28] P. Tzionas, S. Papadakis and D. Manolakis, Plant leaves classification based on morphological features and a fuzzy surface selection technique, in: International Conference on Technology and Automation ICTA'05, pp. 365–370, 2005.
- [29] N. Valliammal and S. N. Geethalakshmi, A novel approach for plant leaf image segmentation using fuzzy clustering, Int. J. Comput. Appl. 44 (2012), 10-20.
- [30] G. K. P. Vyshnavi, M. R. Sirpa, M. Chandramoorthy and B. Padmapriya, Healthy and unhealthy plant leaf identification and classification using hierarchical clustering, Int. Res. J. Eng. Technol. (IRJET) 3 (2016), 448-453.
- [31] W. Xin, Laplacian operator-based edge detectors, IEEE Trans. Pattern Anal. Mach. Intell. 29 (2007), 886-890.
- [32] B. Xing and W.-J. Gao, Fruit fly optimization algorithm, J. Innov. Comput. Intell. 62 (2013), 167-170.